



# Effect of Quartz Particle Size on Sintering Behavior and Flexural Strength of Porcelain Tiles Made from Raw Materials in Uganda



William Ochen<sup>1\*</sup>, Florence Mutonyi Dujanga<sup>2</sup>, Bosco Oruru<sup>2</sup>

<sup>1</sup>Department of Physics, Kyambog University, Kyambogo, Uganda

<sup>2</sup>Department of Physics, Makerere University, Kampala, Uganda

Submitted: December 18, 2018; Published: January 08, 2019

\*Corresponding author: William Ochen, Department of Physics, Kyambog University, Uganda

## Abstract

The objective of this study is to investigate the effect of quartz particle size (QPS) on sintering behavior and flexural strength of porcelain tiles made from raw materials in Uganda. The optimal sintering temperature of samples containing fine (SQ<sub>2</sub>), medium (SQ<sub>3</sub>) and coarse (SQ<sub>4</sub>) QPS, fired at peak temperatures of 1150-1350 °C using a very fast firing rate (60 °C/min) was established. The sintering behavior was analyzed basing on linear shrinkage, water absorption and micrographs of Scanning Electron Microscope (SEM). Phase evaluation was done by X-ray diffraction. The established optimal sintering temperature is 1300 °C, and firing to 1350 °C resulted into bloating as observed by SEM. At 1300 °C, samples containing fine and medium QPS had a value of 0.47% and 0.9% water absorption respectively. ISO 13006 standards classify dry pressed tiles and water absorption as Group BIa and Group BIb respectively, suitable for use as floor tiles. Also, the average flexural strength of 33 MPa, 18 MPa and 8 MPa was exhibited by samples with fine, medium and coarse QPS respectively. The results indicate that samples with fine QPS satisfy the ISO 13006 standards requirement of MPa. The use of fine and medium QPS yielded properties recommended for floor tiles.

**Keywords:** Quartz; Porcelain; Sintering; Flexural Strength

## Introduction

A porcelain tile is a ceramic material made of kaolin clay, feldspar and quartz in the range of 40-50 wt.%, 35-45 wt. % and 10-25 wt. % respectively [1,2]. Improved physical and mechanical properties of porcelain tiles have often been at firing range of 1200-1400 °C, using a fast firing schedule [3]. Typical properties of porcelain tiles are; low water absorption and high flexural strength (>30 MPa). Today, the production of porcelain tiles has increased, and the sales have improved worldwide [4,5]. Their characteristic makes them one of the top commercial products that suit both indoors and outdoors building applications. Due to the complex nature of porcelain system, there are challenges in understanding porcelain in relation to raw materials, processing conditions, phase and microstructure evolution [6]. The role played by each material in a porcelain system is different; kaolin reacts with feldspar and develops mullite crystals after firing. This improves on flexural strength due to interlocking of mullite needles. Feldspar begins to form molten glass at about 980 to 1100 °C, depending on its chemical composition, assisting the sintering process and enabling virtually zero water absorption (7).

Quartz promotes thermal and dimensional stability thus preventing warping. However, for glassy and vitreous materials like porcelain, the principle factor influencing flexural strength

is considered to be quartz particle size [3,6,8,9]. Quartz particle size has a superior effect on flexural strength compared to firing temperature and quartz content<sup>10</sup>. Flexural strength increases with quartz particle size in the range of 10-30 μm [10,11], this is attributed to pre-stressing effect and microstructure evolution [8,11]. According to the pre-stressing theory, the variation in thermal expansion coefficient,  $\alpha$ , between the glassy phase ( $\alpha \sim 3 \times 10^{-6} \text{ K}^{-1}$ ) and un-melted quartz particles ( $\alpha \sim 23 \times 10^{-6} \text{ K}^{-1}$ ) in the temperature range of 20 to 700 °C induces compressive stress on the glassy phase; the compression on the glassy phase improves with quartz particle size. Noteworthy, fine quartz particles dissolve at a faster rate before the larger particles will undergo a major size reduction [3]. This changes the morphology of the pore from large, irregular and interconnected pores formed by coarse quartz particles to small, spherical and isolated pores in fine quartz particles; inter-connected pores are known to act as crack transmitters other than terminators. The flexural strength of porcelains with quartz particle size of μm decrease as the size of the particles is increased. This is attributed to severe fracture around the quartz particle and within the glassy phase [12], and large pores due to low interability.

In Uganda there is only one factory producing ceramic floor tiles. Although there are several deposits [13], no factory

manufactures porcelain tiles. In this study, the raw materials used were got from Ugandan deposits, and processes with varying quartz particle sizes ( $\geq 50\mu\text{m}$ ), to produce porcelain tiles. Evaluation of the properties of the formulated samples was based on ISO 13006 standards. To analyze the sintering behavior, a vitrification curves is used where physical properties (water absorption and linear shrinkage) of the samples is plotted against firing temperature [11]. Sintering curves allow establishment of optimum sintering temperature, usually this corresponds to minimum water absorption or open porosity, and maximum flexural strength and linear shrinkage[1].The aim of this article is to establish the effect of quartz particle size on the sintering behavior and flexural strength of porcelain tiles made using Ugandan raw materials, and also to establish the optimum sintering temperature of samples fired at peak temperature of 1150-1350 °C using a very firing rate of 60 °C/min.

## Materials and Experimental Procedures

### Raw Materials

The raw materials used in this study were obtained from selected deposits in Uganda. Kaolin clay and quartz were got from Mutaka in Bushenyi District. Feldspar was got from Lunya found in Buikwe District. These deposits and their location are described in [13]. Kaolin was dry sieved using a sieve of size 80  $\mu\text{m}$ . Quartz and feldspar were dry milled in a laboratory ball mill (Retsch, PM 100, German) containing twenty-two steel balls as grinding medium. The mill was revolving at 350 rpm for 30 minutes, and after, pulverized feldspar was passed through 50  $\mu\text{m}$  sieve. Quartz particle size was varied using different sieve sizes arranged on a sieve shaker (Retsch, AS 200, German). The mean particle sizes of 50, 90 and 200  $\mu\text{m}$  were obtained, selected on the basis of [12], and classified as shown in (Table 1).

**Table 1:** Classification of Quartz Particle Size.

Quartz Particle Size ( $\mu\text{m}$ )	50	90	200
Classification	fine	medium	coarse
Batch label	SQ1	SQ3	SQ4

### Chemical Analysis of the Raw Materials

The chemical composition of the raw materials was determined by Atomic Absorption Spectrometry (Agilent, 240z/240FSAA), the concentration of the elements present was determined in parts per million (ppm) from where the percentage of their oxides was calculated. The oxides ( $\text{Na}_2\text{O}$ ,  $\text{K}_2\text{O}$ ,  $\text{Fe}_2\text{O}_3$ ,  $\text{CaO}$ ) were determined using flame atomizer whereas electro-thermal atomizer was used for  $\text{SiO}_2$  and  $\text{Al}_2\text{O}_3$ . The results of chemical analysis (Table 2) are expressed in percentage composition of the constituent oxides, and loss on ignition (LOI) was determined as a percentage of change in mass, after 2 hrs of firing at 800 °C.

### Preparation of Porcelain Samples

The weight proportion of the raw materials was typical of traditional porcelain; 50 % kaolin, 30 % feldspar and 20 % quartz. Six kilograms of the mixture was homogenized in a mill

for 1 hour, with plastic balls as the mixing medium. The samples were formulated by cold die pressing using a compression machine (ELE International, England) in a steel mould, and at a pressure of 40 MPa. Rectangular samples measuring 106 x 50 x 7mm were formed from 60 g with 10 wt% moisture content. The green samples were left to dry at room temperature for 72 hour, after they were fired in an electric furnace (CARBOLITE, GERO HTF 1700, German) at peak temperatures (1150-1350 °C) using very fast firing schedule (60 °C/min), and soaked for 1 hr. After firing, the samples were left to cool naturally in the furnace.

## Experimental Measurements

### Linear Shrinkage

The linear shrinkage of the samples was calculated using (Equation (1)) [14,1]. A total of five samples were used for each peak temperature from which the average value was calculated.

$$L.S(\%) = \left[ \frac{D_g - D_f}{D_g} \right] \times 100 \quad (1)$$

where  $D_g$  and  $D_f$  are dimensions in millimeters of the dry and fired samples respectively, measured using a digital venire caliper.

### Water Absorption

The water absorption was measured using liquid displacement method according to Archimedes principle (ASTM C373-88). The masses of the dry samples ( $m_1$ ) were measured using a digital electronic balance. The samples were then boiled in distilled water for 2 hours, and soaked for 24 hours at room temperature. After impregnation, the mass of the saturated samples ( $m_2$ ) was measured. Five samples were used at every peak temperature from where the average value of water absorption was calculated. Water absorption, calculated using (Equation (2)) [14,1], expresses the relationship of the mass of water absorbed to mass of the dry samples.

$$W (\%) = \frac{m_2 - m_1}{m_1} \times 100 \quad (2)$$

### Flexural Strength/Modulus of Rupture (MOR)

The flexural strength of the samples was determined by three-point loading method (using Ametek, Lloyd Instrument, UK). The span length (L) considered in the measurement was 100 mm. A force (F) loading at a rate of 0.5 mms<sup>-1</sup> was directed to the center of the samples, and upon breaking of the test sample its value was noted. A total of seven samples were considered at every peak temperature from which the average value of MOR was calculated using (Equation (3)) [15].

$$MOR = \frac{3FL}{2bt^2} \quad (3)$$

Where  $b$  and  $t$  are breadth and thickness respectively of the samples measured using a digital venire caliper in millimeters.

### Microstructure and Phase Analysis

The microstructures of the samples at optimum sintering temperature were characterized using CARL ZEISS Scanning Electron Microscope (SEM) instrument, EVO MA 10. Sectioned and polished specimens of the fired samples were used for the investigation. The specimens were polished, cleaned and dried. Thereafter, they were dipped in 40% concentrated hydrofluoric acid for 25 s, cleaned, dried and studied using CARL ZEISS instrument. The cleaning procedures given to all specimens before examination included washing in water and alcohol before drying.

The crystalline phases in the fired porcelain samples were determined by X-ray diffraction using an X'pertPRO PAN alytical X-ray diffractometer, PW 3050/60, with Ni-filtered  $K\alpha$  Cu-radiation generated by a 40kV acceleration voltage and a 40 mA anode current. Pulverized specimens were scanned from 10 to 90° operating the equipment at a 2θ scan-speed of 0.5 sec/step and a 2θ step size of 0.02°. The X-ray peaks of the different phases were identified with HighScore software

### Results and Discussion

#### Chemical Composition

Chemical analysis was done on all the raw materials used in the study, and results are given in Table II. The raw materials were got from selected deposits and processed for chemical analysis with no additives.

**Table 2:** Chemical Analysis (%) of the Raw Materials.

Composition (%)	Kaolin	Feldspar	Quartz
SiO <sub>2</sub>	53.41	62.82	99.59
Al <sub>2</sub> O <sub>3</sub>	35.64	17.23	
Fe <sub>2</sub> O <sub>3</sub>	0.03	0.14	0.04
Na <sub>2</sub> O	0.04	0.30	0.04
K <sub>2</sub> O	0.01	4.23	0.02
C <sub>a</sub> O	0.28	0.29	0.39
Others	0.63	17.5	
LOI	9.96	1.49	0.34

Kaolin, quartz and feldspar were of common type used in porcelain. The percentage of SiO<sub>2</sub> and Al<sub>3</sub>O<sub>3</sub> are within range reported for porcelain manufacture. The fluxing oxide is K-feldspar, due to high percentage of K<sub>2</sub>O present compared Na<sub>2</sub>O and CaO. However, the percentage of K<sub>2</sub>O is low in this case as compared to that reported by other workers [16,1,13]. This is attributed to processing technique, as the material was not washed or soated to remove impurities such as quartz. The material was milled as got from the deposit. The alkali oxide plays a significant role towards densification, by forming a vitreous phase that blocks the open pores present in the microstructure. On the same note, they contribute towards phase transformation, mullite formation where their presence in the porcelain body enhances mechanical strength [17]. The lower flux oxide probably explains the high optimum sintering

temperature of 1300 °C exhibited in this study, similar work reported a value of 1250 °C [13]. The small amount of impurities such as Fe<sub>2</sub>O<sub>3</sub> is recommendable, so as to avoid coloring pollution of the samples, and to minimize defects such as bloating [18]. In this study, other oxides such as P<sub>2</sub>O<sub>3</sub>, MgO, MnO and TiO<sub>2</sub> were not analyzed, since similar work reported negligible amount [13], and the researcher has not come across any literature relating their effect on flexural strength.

#### Linear Shrinkage

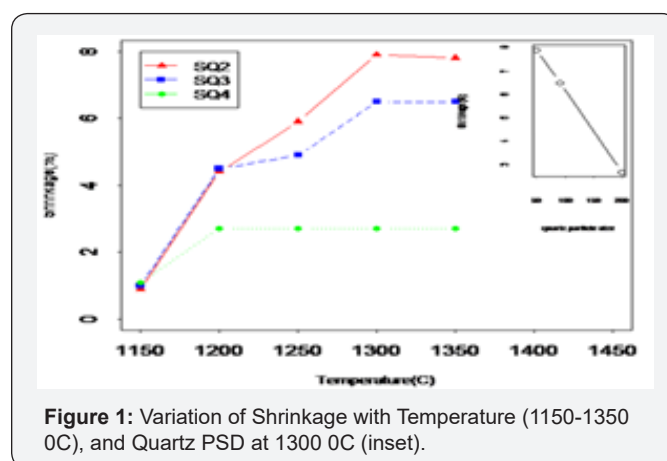


**Figure 1:** Variation of Shrinkage with Temperature (1150-1350 °C), and Quartz PSD at 1300 °C (inset).

The shrinkage behavior of porcelain products during sintering is important, because it allows controlling the dimensions of the final product [4]. The shrinkage of the samples was plotted against the firing temperature. (Figure 1) displays a general increase in shrinkage as temperature raises from 1150-1300 °C. The results show a similar value of shrinkage (~0.8%) by all the batches at 1150 °C, and for batches SQ<sub>2</sub> and SQ<sub>3</sub> (4.6%) at 1200 °C. Further increase in shrinkage at 1300 °C, and slight decline at 1350 °C was exhibited by SQ<sub>2</sub> and SQ<sub>3</sub>. Batch SQ<sub>4</sub> exhibited shrinkage of 2.8% at 1200 °C; firing further yielded no change in the shrinkage. The maximum shrinkage for all batches (7.9%) was exhibited by SQ<sub>2</sub>. Noteworthy, the shrinkage of the samples decreases with increasing quartz particle size (Figure 1). The discussions in this study were focused on batches with fine and coarse quartz particle size because of the distinct nature of their results.

The increase in shrinkage with temperature is attributed to the diminishing of particles as they approach fusion. The particles melt as temperature increase further and the viscosity of the melted glassy phase formed decreases as temperature rises. Therefore, when the body cools, particles pull together leading to increase in shrinkage [19]. The high shrinkage means that more thermal changes occurred within the raw materials, and this behavior is fostered by increasing temperature [4]. However, above 1300 °C, as the melted glassy substance becomes less viscous, bubble begin to form due to escape of entrapped gasses, and shrinkage of the samples reduces due to increase in total porosity. Most cases bubbles develop when samples are fired beyond their optimum temperature. This will be discussed later in microstructure observation.

The shrinkage of the samples reduced as the size of quartz particles increased. This behavior is typical of porcelain materials [20]. During sintering, the presence of fine quartz particles increases the amount of silica content in the liquid phase, which fills the pores and promotes bringing closer the particles. Fine quartz particles dissolve faster because more of their surface area is exposed to the liquid phase emanating from feldspar8 fostering shrinkage. Subsequently, low shrinkage noticed by using coarse quartz particles is attributed to low rate of dissolution, which reduces the amount of glassy phase therefore creating large pores in the microstructure [21]. At 1150 °C no variation in shrinkage is noticed as quartz particle size changes probably because quartz dissolution had not started yet.

### Water Absorption

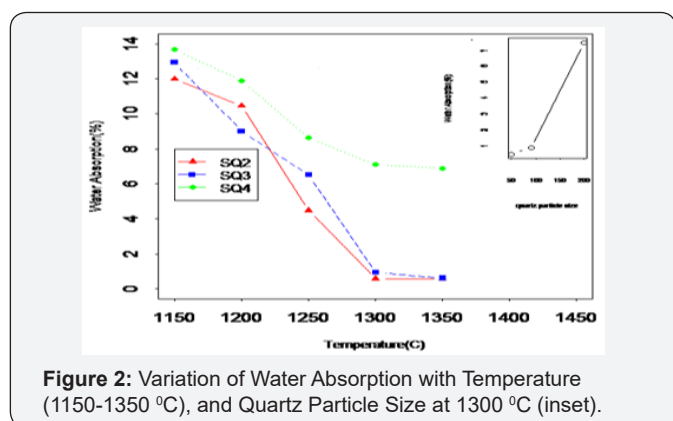


Figure 2: Variation of Water Absorption with Temperature (1150-1350 °C), and Quartz Particle Size at 1300 °C (inset).

Water absorption defines the durability and the class to which the final porcelain product belongs4. The water absorption reduced with increase in firing temperature from 1150-1300 °C, and at 1350 °C no significant change was observed (Figure 2), this trend is typical of porcelain materials3. Batches SQ<sub>2</sub> and SQ<sub>3</sub> exhibited almost the same behavior at all temperatures, and SQ<sub>4</sub> had higher values ranging from ~6 to ~13 % (Figure 2). (inset) shows how water absorption varies with quartz particle size at 1300 °C. In addition, it is observed that at 1300 °C batches with fine quartz particle size had a value of ~0.47% which is less than 0.5%. According to (ISO 13006 standards), this type of porcelain ware are recommended for use as floor tiles.4 Standards (ISO 13006) further classifies dry pressed tiles with ≤0.5% with water absorption as Group BIb, SQ<sub>2</sub> and SQ<sub>3</sub> whose value is~0.9% qualify, and are recommended for use as floor tiles. However, 6-10% is classified as Group BIII, and SQ<sub>4</sub> with ~7.1% lies in this range. These are not suitable for flooring [22].

The water absorption decreases with increase in firing temperature. This observation is a result of good densification of the samples9. At about 1100 °C, K-feldspar starts melting to form a liquid phase that surrounds the particles [2]. The capillary pressure created at the contact points binds the particles closer while altering pore size and shape, hence lowering water absorption. Further increase in temperature, promotes the difference in the viscosity of the liquid formed and contributes to decrease in pore size and hence further reduction in water absorption [23].

Batches with fine quartz particle size distribution exhibited lower water absorption than coarse particles. This is because raising the quartz particle size leads to larger quantities of un melted quartz grains due to low sintering thereby increasing the size of the pores [24]. It is known that, due to non plastic nature of quartz, it disperses in the green body containing voids between clay platelets. After sintering, pores of the size related to the non plastic material are formed. This connects well with the rise in water absorption as the quartz particle size was increased. On the other hand, fine quartz particles melt away easily, increasing the glassy phase, and forming smaller, regular and isolated pores in the microstructure. This signifies high degree of liquid phase sintering, and densification. Preferably explaining low water absorption exhibited, similar results were obtained by12. In this study, the sintering behavior of the fired samples was evaluated by linear shrinkage and water absorption1, and the optimum sintering temperature was achieved when water absorption reached a minimum value, tending to zero, and simultaneously linear shrinkage is maximum. This occurred for samples fired at 1300 °C. At 1350 °C, bubbles started to appear in the microstructure of the fired samples.

### Flexural Strength/Modulus of Rupture (MOR)

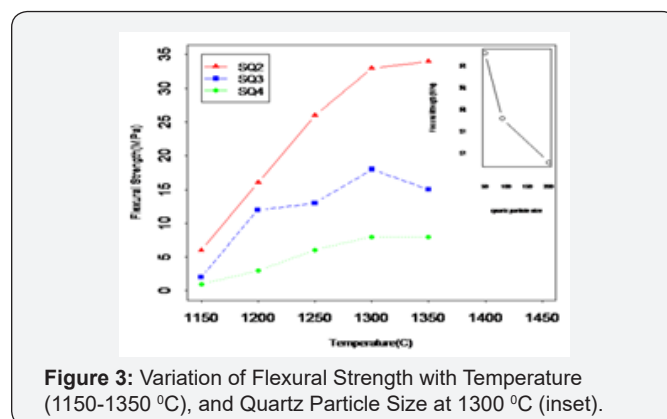


Figure 3: Variation of Flexural Strength with Temperature (1150-1350 °C), and Quartz Particle Size at 1300 °C (inset).

The flexural strength of the samples containing different quartz particle sizes and fired at different temperature is given by (Figure 3). The results illustrate that the flexural strength increases with firing temperature (1150-1300 °C) and decreases when the quartz particle size is increased (Figure 3). At 1300 °C, the average flexural strength values of fine (SQ<sub>2</sub>) and medium (SQ<sub>3</sub>) particles are 33 MPa and 18 MPa respectively. Also, the samples with coarse quartz particle size (SQ<sub>4</sub>) presented the lowest flexural strength of ~8Mpa. The results indicate that samples with fine quartz particle size satisfies the ISO 13006 standards requirement of MPa [4].

The increase in strength with temperature is attributed to the reactions that occur during the sintering process, such as elimination of pores and formation of crystalline phases like mullite [23]. Increasing temperature eliminated open pores by viscous flow, which is controlled by melt viscosity. The melt viscosity is directly related to the particle size of quartz, a dense microstructure is achieved by decreasing the quartz particle size. Since the powers of fine sized quartz particles are higher

than those of coarse quartz particles, their mobility is also higher thus they can react easily and increase the speed of sintering [25]. Another important issue is particle packing density after pressing; this is controlled by particle size of the material being processed. Fine quartz particles have a higher packing density than coarse particles. The diffusion distance of the particles can be shortened to increase sintering speed with dense packing. As a result the flexural strength values of the fired samples decrease.

On the other hand, the increase in flexural strength is also attributed to mullite content, according to mullite hypothesis<sup>10</sup>, mullite crystals act as a re-enforcement to the glassy phase. The mullite content is enhanced by fine size of the quartz particles<sup>9</sup>. Recently, Güngör (25) investigated the influence of quartz particle size on the mechanical strength of porcelain. The author reported that the amounts of secondary mullite crystals are increased by decreasing the particle size of quartz and increasing the temperature. In conclusion, flexural strength is improved by reducing the size of quartz particles, because the mullite content is improved at elevated temperature.

### Microstructure and Phase Analysis

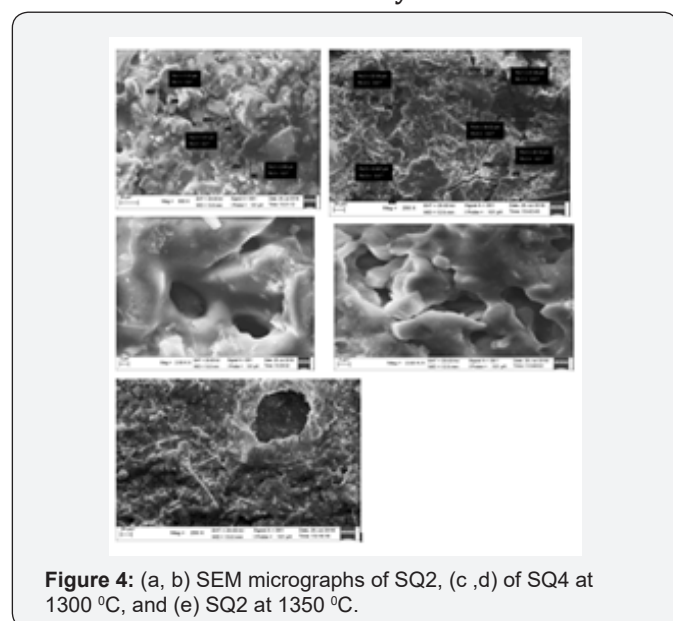


**Figure 4:** (a, b) SEM micrographs of SQ2, (c, d) of SQ4 at 1300 °C, and (e) SQ2 at 1350 °C.

The Scanning Electron Microscope (SEM) micrographs of samples fired at 1300 °C with fine and coarse quartz particle sizes are represented by (Figure 4a-d). Comparing micrographs, it is observed that quartz particle size influences the microstructure evolution of the final product. The sintered body with coarse quartz particle size (Figure 4b) shows a rough and granular texture [26]. This probably shows un-melted quartz grains. As a result of low sintering, large pores in the range of 11 to 34 μm were formed by coarse particles, relating to high water absorption (~7.1%). The samples with fine quartz particles exhibited a higher degree of glassy phase forming smooth surface, compacted texture and dense micro structure (Figure 4a), relating to low water absorption (~0.47%) and high flexural strength (33 MPa). The small pores of size 3-10 μm formed by

fine quartz particles, emphasizes high degree of liquid formation as fine quartz particles are known to dissolve faster [3].

On the same note, due to high viscosity of the glassy phase by coarse quartz particles, there is a delay in the homogenization of the texture, this may be the reason for large, irregular and interconnected nature of the pores [27] (Figure 4d). Mostly, this signifies low degree of liquid formation probably as a result of very high sintering rate (60 0C/min) used in this study, and the low dissolution behavior of coarse quartz particles. Interconnected pores are detrimental because they facilitate crack propagation thereby decreasing flexural strength<sup>16,8</sup>, relating to ~8 MPa obtained in this study. Likewise, spherical and isolated pores in samples with fine quartz particles (Figure 4c) relates to densification (<0.5% water absorption). This characterizes the final stage of sintering<sup>16</sup>. Isolated pores are known to act as termination points for crack propagation, enhancing flexural strength.

The slight decline in flexural strength and shrinkage of samples fired beyond 1300 0C was attributed to a defect known as bloating (Figure 4e). Expulsion of gasses (bloating) occurs in the liquid phase at higher temperature leading to increase in total porosity [23] or water absorption in this case. The origin of bloating in the liquid substance can be associated with the loss of the hydroxyl group in the kaolinitic mineral and more severely during the release of oxygen due to the decomposition of Fe<sub>2</sub>O<sub>3</sub> to Fe<sub>3</sub>O<sub>4</sub> [8]. However, it is reported that bloating is not a heating rate effect, but it occurs when samples are fired beyond the optimum temperature [27].

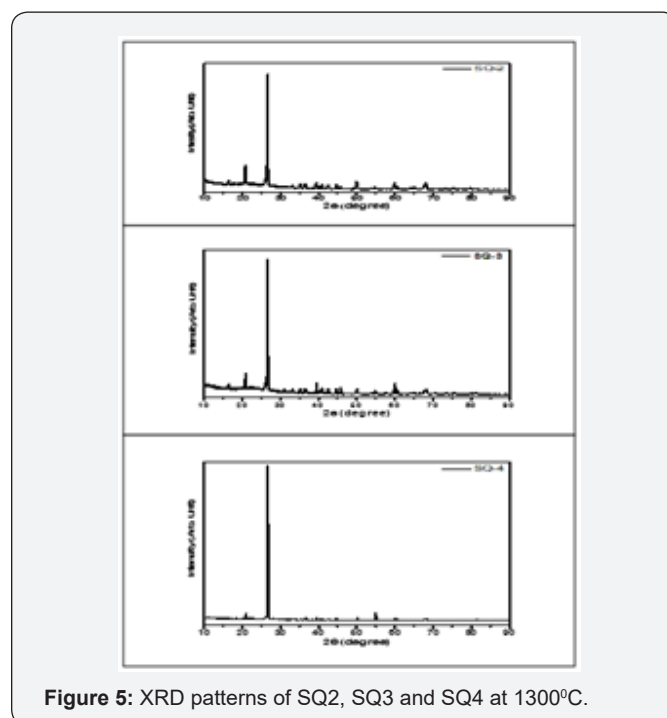


**Figure 5:** XRD patterns of SQ2, SQ3 and SQ4 at 1300°C.

X-ray diffractograms of different batches fine (SQ<sub>2</sub>), medium (SQ<sub>3</sub>) and coarse (SQ<sub>4</sub>) fired at 1300 °C are illustrated in (Figure

5). It can be noted that the principle crystalline phase present is quartz, represented by highest intensity peak at 20~250. It can be seen that the intensity of the quartz peaks increases in parallel with increase of the quartz particle size, which indicates low dissolution of coarse quartz particles [9].

### Conclusion

In this study, the effect of using different quartz particle sizes on the sintering behavior and flexural strength of porcelain tiles has been investigated. The SEM analysis revealed isolated and spherical pores for samples with fine quartz particle sizes, irregular and interconnected pores for coarse quartz particle size that enhanced the increase of water absorption and decrease in flexural strength. The flexural strength of samples increased from 8, 18 and 33 MPa at 1300 °C for coarse, medium and fine quartz particle size respectively. These results indicate that samples with fine quartz particle size satisfy the ISO 13006 standard requirement of MPa. Also, samples with fine and medium quartz particle size exhibited water absorption of 0.47% and 0.9% respectively. The ISO 13006 classifies water absorption as Group BIa, recommends use as floor tiles.

### References

- Martín Márquez J, Rincón J M, Romero M (2008) Effect of firing temperature on sintering of porcelain stoneware tiles. *Ceram Int* 34: 1867-1873.
- Sanz V, Moreno A, Sa E (2010) Porcelain tile: Almost 30 years of steady scientific technological evolution. *Ceram Int* 36: 831-845.
- Turkmen O, Kucuk A, Akpınar S (2015) Effect of wollastonite addition on sintering of hard porcelain. *Ceram Int* 41: 5505-5512.
- Njindam OR, Nyoya D, Mache JR, Mouafon M, Messan, et al. (2018) Effect of glass powder on the technological properties and microstructure of clay mixture for porcelain stoneware tiles manufacture. *Constr Build Mater* 170: 512-519.
- Abadir MF, Sallam EH, Bakr IM (2002) Preparation of porcelain tiles from Egyptian raw materials. *Ceram Int* 28: 303-310.
- Dana K, Das S, Das SK (2004) Effect of substitution of fly ash for quartz in triaxial kaolin quartz feldspar system. *J Eur Ceram Soc* 24: 3169-3175.
- Cam WM, Senapati U (1998) Porcelain Raw Materials Processing Phase Evolution and Mechanical Behavior. *J Am Ceram Soc* 81(1): 3-20.
- Kobayashi Y, Ohira O, Ohashi Y, Kato E (1992) Effect of Firing Temperature on Bending Strength of Porcelains for Tableware. *J Am Ceram Soc* 75: 1801-1806.
- Boussouf L, Zehani F, Khenioui Y, Boutaoui N (2018) Effect of Amount and Size of Quartz on Mechanical and Dielectric Properties of Electrical Porcelain. *Trans Indian Ceram Soc* 77: 132-137.
- Stathis G, Ekonomakou A, Stournaras CJ, Ftikos C (2004) Effect of firing conditions, filler grain size and quartz content on bending strength and physical properties of sanitaryware porcelain. *J Eur Ceram Soc* 24: 2357-2366.
- Ece OI, Nakagawa ZE (2002) Bending strength of porcelains. *Ceram Int* 28(2): 131-140.
- Warsaw SI, Seider R (1967) Comparison of Strength of Triaxial Porcelains Containing Alumina and Silica. *J Am Ceram Soc* 50: 337-343.
- Olupot PW, Jonsson S, Byaruhanga JK (2010) Development and characterisation of triaxial electrical porcelains from Ugandan ceramic minerals. *Ceram Int* 36: 1455-1461.
- Mahdi O S (2018) Study the Influence of Sintering on the Properties of Porcelain Stoneware Tiles. *Inter Journal of Applied Engineering and Research* 13: 3248-3254.
- Lee VG, Yeh TH (2008) Sintering effects on the development of mechanical properties of fired clay ceramics. *Mater Sci Eng* 485(1-2): 5-13.
- Amorós JL, Orts MJ, Mestre S, Garcia Ten J, Feliu C, et al. (2010) Porous single fired wall tile bodies: Influence of quartz particle size on tile properties. *J Eur Ceram Soc* 30(1): 17-28.
- Iqbal Y, Lee WE (2000) Microstructural evolution in triaxial porcelain. *J Am Ceram Soc* 83: 3121-3127.
- Kitouni S, Harabi A (2011) Sintering and mechanical properties of porcelains prepared from algerian raw materials. *Cerâmica* 57: 453-460.
- Salem A, Jazayeri SH, Rastelli E, Timellini G (2010) Thermochemical Kinetic model for isothermal sintering of porcelain stoneware body in presence of nepheline syenite. *Thermochim Acta* 503(1): 1-7.
- Souza GP, Messer PF, Lee WE (2006) Effect of varying quartz particle size and firing atmosphere on densification of Brazilian clay-based stoneware. *J Am Ceram Soc* 89: 1993-2002.
- Bragança S R, Bergmann CP (2006) Effect of Quartz of Fine Particle Size on Porcelain Properties. *Mater. Sci Forum* 530-531: 493-498.
- Romero M, Pérez JM (2015) Relation between the microstructure and technological properties of porcelain stoneware. A review *Mater construcción* 65: 1-19.
- Gralik G, Chinelatto AL, Chinelatto ASA, Grossa P (2014) Effect of different sources of alumina on the microstructure and mechanical properties of the triaxial porcelain. *Ceramica* 60(356): 471-481.
- Quereda MF, Hutchings IM, Xu Y, Sanchez E, Ibanez MJ, et al. (2006) Porcelain tile microstructure: implications for polishability. *J Eur Ceram Soc* 26: 1035-1042.
- Güngör, F, Ay N (2018) The effect of particle size of body components on the processing parameters of semitransparent porcelain. *Ceram Int* 44(9): 10611-10620.
- Mukhopadhyay TK, Ghosh S, Ghatak S, Maiti HS (2006) Effect of pyrophyllite on vitrification and on physical properties of triaxial porcelain. *Ceram Int* 32(8): 871-876.
- Lerdprom, W, Chinnam RK, Jayaseelan DD, Lee WE (2016) Porcelain production by direct sintering. *J Eur Ceram Soc* 36: 4319-4325.



This work is licensed under Creative Commons Attribution 4.0 License  
DOI: [10.19080/JOJMS.2019.05.555661](https://doi.org/10.19080/JOJMS.2019.05.555661)

### Your next submission with Juniper Publishers will reach you the below assets

- Quality Editorial service
- Swift Peer Review
- Reprints availability
- E-prints Service
- Manuscript Podcast for convenient understanding
- Global attainment for your research
- Manuscript accessibility in different formats  
**( Pdf, E-pub, Full Text, Audio)**
- Unceasing customer service

Track the below URL for one-step submission  
<https://juniperpublishers.com/online-submission.php>